von Willebrand Factor D and EGF Domains is an evolutionarily conserved and required feature of blastemas capable of multi-tissue appendage regeneration

Leigh N.D.[1,2], Sessa S.[1], Dragalzew A.C.[3], Payzin-Dogru D.[1], Sousa J.F.[3], Aggouras A.N.[1], Johnson K.[1], Dunlap G.S.[1], Haas B.J.[2] , Levin M.[4,5], Schneider I.[3], Whited J.L.[1,2,4]

Affiliations:

[1]Department of Stem Cell and Regenerative Biology, Harvard University, 7 Divinity Ave. Cambridge, MA, 02138, USA

[2]Broad Institute of MIT and Harvard, 7 Cambridge Center, Cambridge, MA, 02142, USA

[3]Instituto de Ciências Biológicas, Universidade Federal do Pará, 66075-900 Belém, Brazil

[4]Allen Discovery Center at Tufts University, Tufts University, Medford, MA, 02155, USA

[5]Department of Biology, Tufts University, Medford, MA 02155, USA

Abstract

Regenerative ability varies tremendously across species. A common feature of regeneration of appendages such as limbs, fins, antlers, and tails is the formation of a blastema--a transient structure that houses a pool of progenitor cells that regenerate the missing tissue. We have identified the expression of *von Willebrand Factor D and EGF Domains* (*vwde*) as a common feature of blastemas capable of regenerating limbs and fins in a variety of highly regenerative species. Further, *vwde* expression is tightly linked to the ability to regenerate appendages. Functional experiments demonstrate a requirement for *vwde* in regeneration and indicate that Vwde is a potent mitogen in the blastema. These data identify a key role for *vwde* in regenerating blastemas and underscore the power of an evolutionarily-informed approach for identifying conserved genetic components of regeneration.

Introduction

The underlying reasons why some animals have the ability to regenerate complex structures, while others cannot, remains an important and open question. This knowledge gap has led to intense study of how regeneration-competent species are able to perform complex multi-tissue regeneration, with a particular focus on the ability to regenerate paired appendages, such as limbs and fins. However, this has long been a pursuit without an understanding of whether this ability was present when paired appendages first evolved or was acquired by certain phylogenetic lineages (e.g. urodele amphibians).

Recent work regarding the evolutionary origins of regenerative capacity has indicated that the ability to regenerate paired appendages is an inherited feature of the fin-to-limb transition [1–4]. Evidence found in the fossil record [3,4], functional studies across species [2], and comparisons of gene expression profiles of regenerating tissue [1,2] support the notion that paired appendage regeneration is a feature lost by certain lineages and was not a newly derived capacity in highly regenerative lineages. This indicates that the amniote lineage (which includes humans) has lost regenerative tendencies in appendages over evolutionary time. Therefore, the ability to stimulate regeneration in non-regenerative species, potentially in a therapeutic context, may require the re-initiation of a core, evolutionary conserved program.

All species that are able to regenerate appendages share a conserved trait: the ability to form a blastema. The blastema is the morphological structure that forms at the amputation plane and houses the progenitor cells responsible for regeneration. Recent efforts have focused on elucidating the molecular definition of the blastema, with many of these efforts aimed at the axolotl limb blastema due to the ease of tissue acquisition and the ability to perform experimentation in the lab [5–13]. These studies provide a wealth of information about transcriptomic changes over time, cell types, and blastema-enriched genes. More recently,

55 sequencing efforts of non-model species have allowed for comparisons to the axolotl limb
56 blastema and indicate a core molecular signature that is shared between the blastemas of
57 distantly related species [1,2]. Due to these similarities and the common evolutionary origin of
58 limb regeneration capacity, we can use an evolutionarily-informed approach to understand what
59 constitutes a blastema and for identifying core features required for regeneration.

60 A recent approach to identify the unique gene expression in the axolotl limb blastema
61 compared blastema gene expression to a variety of homeostatic and embryonic tissues and
62 identified over 150 blastema-enriched genes [11]. These blastema-enriched genes may help to
63 explain the unique functions of the blastema, but the question remains as to whether these genes
64 represent a core program or are functionally required for regeneration. One of the most blastema-
65 enriched genes in this dataset was *von Willebrand Factor D and EGF Domains* (*vwde*), which to
66 date has not been functionally studied in any context.

67 We decided to apply an evolutionary framework to determine if *vwde* fit the description
68 of an evolutionary-conserved, blastema-enriched gene and if such an approach may help to
69 identify genes required for regeneration. We found that *vwde* expression is a common feature of
70 both fin and limb blastemas and was highly enriched in regenerating appendages as compared to
71 pre-amputation intact appendages. In addition, using the natural regeneration-competent and
72 regeneration-refractory periods during *Xenopus laevis* development, we observed that *vwde*
73 expression was tightly linked to the regeneration-component environment. This suggests that
74 *vwde* may be a critical factor in the regenerative niche. Finally, we found that *vwde* is
75 functionally required for axolotl limb regeneration, with transient knockdown of protein levels
76 resulting in aberrant regeneration. These data suggest that an evolutionarily-informed approach

77 can help to prioritize target genes and that genes that are blastema-enriched across different
78 species may prove to be critical factors in the ability to regenerate appendages.
79
80
81 **Results**
82 With the goal of identifying genes enriched to the regenerating blastema, a tissue-mapped
83 axolotl transcriptome was recently published [11]. Of particular interest are blastema-enriched
84 genes with high expression in the blastema and relative low expression in all other tissues
85 sampled. We found that *vwde* was highly enriched to the axolotl limb blastema (Figure 1A). This
86 analysis, however, was limited to one time point, the medium-bud blastema, and it did not
87 provide spatial information about the expression of *vwde* across the regenerating limb. To
88 understand the spatial and temporal regulation of *vwde*, we performed RNA *in situ*
89 hybridizations over a time course of axolotl limb regeneration. We found *vwde* expression to be
90 tightly tied to the presence of a blastema and expressed exclusively in the blastema and not the
91 overlying wound epidermis (Figure 1B-E). Thus, *vwde* fits the description of an axolotl limb
92 blastema-enriched gene and we were interested in pursuing whether *vwde* may be a core
93 component of blastemas able to regenerate appendages.
94 We next sought to determine if *vwde* was present in a selection of deuterostomes,
95 including species with various regenerative abilities. Using a comparative genomics approach
96 [14], we found *vwde* to have orthologs across deuterostomes (though no ortholog was detected in
97 *Ciona intestinalis*), as well as a non-blastema-enriched paralogous gene in axolotl and other
98 species (Figure 1F, Supplementary Figure 1). Comparing protein domain composition, we find
99 that Vwde from all species sampled had von Willebrand Factor D domains and EGF-like

100 domains, the latter of which varied more substantially across species in terms of number of
101 domains. This analysis indicates that *vwde* is present in both amniotes and anamniotes, but based
102 on the species used in this analysis, Vwde is truncated with loss of either all or some of the EGF-
103 like domains in amniotes (Figure 1F). Using these identified orthologs, we moved forward to ask
104 whether *vwde* was a blastema-enriched gene during paired fin regeneration.

105 We explored the possibility that *vwde* could be a common feature of blastemas
106 responsible for regenerating paired fins, which share a deep homology with limbs [15], and
107 likely share an inherited gene regulatory program for regeneration [1,2]. We chose two highly
108 regenerative, but distantly related, fish species to determine if *vwde* expression was a conserved
109 feature of blastemas capable of regenerating paired appendages. These include a species in the
110 sister group to tetrapods, the Lungfish (*Lepidosiren paradoxa*), which is a lobe-finned fish, and
111 *Polypterus senegalus*, a ray-finned fish that is capable of regenerating after amputation through
112 skeletal elements that develop by endochondral ossification. We first inspected publicly available
113 transcriptome datasets of lungfish and *Polypterus* regenerating fins for the *vwde* orthologs we
114 previously identified (Figure 1F). The lungfish LG29893_g1_i1 contig was upregulated in
115 blastemas 21 days post-amputation (dpa) relative to uninjured fins [1], and the *Polypterus*
116 PS64836c0_g1_i1 contig was upregulated in 9 dpa blastemas relative to uninjured fins [2].
117 Assessment of expression levels via qPCR at various regeneration stages showed an upregulation
118 of *vwde* coinciding with blastema formation during lungfish fin regeneration (Supplemental
119 Figure 2A).

120 A similar pattern was seen for *Polypterus* fin regeneration, with expression reaching
121 highest levels at 5 dpa (Supplemental Figure 2B). Next, we assessed the spatial pattern of *vwde*
122 in histological sections of regenerating fins. Lungfish 21 dpa blastemas show distal

123 mesenchymal expression of *vwde* (Figure 2A). In 5 dpa *Polypterus* blastemas, expression is
124 observed distal to the amputation plane in mesenchymal cells but also in the epithelium,
125 suggesting that *Polpyterus* may use *vwde* in both compartments (Figure 2C). *In situ* hybridization
126 with control sense probes did not yield specific signal (Supplemental Figure 2C-D).
127 Histologically, these samples are similar to the medium-bud blastema time point in which we
128 identified *vwde* in the axolotl limb (Figure 2B, 2D). Together, these data indicate that *vwde* is
129 expressed in regenerating fins and limbs and that *vwde* expression is a conserved feature of
130 blastemas.

131 To further investigate *vwde* during regeneration, we took advantage of the regeneration-
132 competent and regeneration-refractory periods during *Xenopus laevis* tail development [16]. A
133 blastema forms in response to amputation during both distinct developmental stages, but only in
134 the regeneration-competent setting is full regeneration accomplished. This developmental feature
135 provides an ideal situation to compare regeneration-component versus regeneration-refractory
136 environments. We reasoned that finding factors that differentiate these two contexts may provide
137 clues for identifying the core requirements for successful regeneration. We probed for the
138 expression of *vwde* during the regeneration-competent and regeneration-refractory periods of
139 *Xenopus laevis* tail regeneration. Interestingly, we found that *vwde* expression was present in
140 tails prior to amputation in both the regeneration-competent and regeneration-refractory setting
141 (Figure 3A-B, 3G-H). We found robust *vwde* expression along the peripheral edge of the
142 amputation plane and near the blastema in regeneration-competent tails (Figure 3C-F). In
143 contrast, in the regeneration-refractory setting, *vwde* expression was restricted to the peripheral
144 edges of the amputation plane and was not detected near the blastema (Figure 3I-L). This
145 indicated a striking correlation between *vwde* expression and regeneration, providing evidence

146 that *vwde* may be an important factor in forming a pro-regenerative niche. These expression data
147 across a range of species indicate that *vwde* fits the profile of an evolutionarily-conserved,
148 regeneration-enriched gene and that *vwde* may play an important role in the blastema niche.
149 To investigate if *vwde* is required for regeneration, we performed morpholino-mediated
150 knockdown at its peak expression in the medium-bud limb blastema. We found a substantial
151 reduction in the length of the blastemas when Vwde was knocked down with two separate
152 translation-blocking morpholinos (Figure 4A-B). Fluorescent reporter constructs with *vwde*-
153 morpholino binding sites confirmed that both unique *vwde*-targeting morpholinos were capable
154 of blocking translation (Supplemental Figure 3). Due to the dramatic reduction in blastema
155 length, we investigated if *vwde* was important for blastema proliferation and/or cell survival. We
156 found that knockdown of Vwde substantially reduced blastema cell cycle entry (Figure 4C-D)
157 and did not alter cell survival compared to control limbs (Supplemental Figure 4). Due to the
158 observed delay in blastema growth, we questioned whether blastemas treated with translation-
159 blocking morpholinos were capable of recovering from the transient knockdown of Vwde and
160 produce fully regenerated limbs. We therefore performed the same Vwde morpholino-mediated
161 knockdown on a separate group of axolotls, and then allowed for the full course of regeneration
162 to complete, harvesting limbs more than eight weeks post-amputation. We observed that one-
163 time injection of Vwde-targeting morpholino caused substantial abnormalities in regenerated
164 limbs, suggesting an essential role for *vwde* during limb regeneration (Figure 4E-G). We found
165 defects in 4.2% (1/24) control limbs compared to 46% (13/28) of limbs treated with *vwde* MO1
166 and 25% (5/20) of limbs treated with *vwde* MO2 (Fisher's exact test $P < 0.05$) (Figure 4F, Table
167 1, Supplemental Figure 5). A second experiment yielded similar results, with defects at endpoint
168 in 27.6% (8/29) of control (*vwde* MO1 inverted) treated limbs compared to 47% (18/38) of limbs

169 treated with *vwde* MO1 (Fisher's exact test $P < 0.05$) (Figure 4G, Table 2, Supplemental Figure
170 6). We found a variety of defects, some of which are reminiscent of limb development
171 phenotypes where limited distal elements are present such as has been observed in *fgf4,8*-double-
172 knockout mice [17] and in the absence of *sonic hedgehog* (*ssh*) [18]. In addition, these
173 phenotypes also resemble the defective regenerative spike characteristic of *Xenopus* limb
174 regeneration [19]. Altogether, these data highlight the functional requirement for *vwde* during
175 limb regeneration.
176
177 **Discussion**
178 Recent work, most notably next generation sequencing, has led to a plethora of
179 information about the genes and cells that define the blastema [1,2,5–13]. However, it is difficult
180 to determine which genes may have functional relevance based purely on their expression. We
181 decided to investigate a single blastema-enriched gene, *vwde*, using an evolutionarily-informed
182 approach, assuming that a gene whose expression is enriched in blastemas of multiple, distantly-
183 related, species is likely a key factor during regeneration.
184 The *in vivo* assays used here place Vwde as a critical regulator of cell cycle entry during
185 axolotl limb regeneration. Proliferation is a complex, but fundamental, aspect of regeneration, as
186 there are many different cell types and potential origins of proliferative signals. Previous work
187 indicates that mitogenic signals are produced directly following amputation independent of the
188 nerve or wound epidermis [20,21], but are also provided by the nerve [22,23] or wound
189 epidermis [24]. There are thus multiple sources of mitogenic signals in the regenerating limb, but
190 it is unclear if mitogenic signals from multiple tissues are required simultaneously or perhaps in
191 a more stepwise fashion to maintain blastema proliferation. Our data indicate that Vwde may be
192 a blastema progenitor cell-derived mitogen, which adds to the potential sources of proliferative

193 signals in the regenerating limb. It has been previously postulated that nerve-derived signals are
194 required early on during blastema formation and growth, but a fibroblast-derived factor is
195 required for complete regeneration [25]. We speculate that *vwde*, which appears to be expressed
196 across the majority of cells in the blastema including likely fibroblasts, may provide one of the
197 essential fibroblast-derived factors required after the nerve has provided sufficient input. While
198 there is limited knowledge of fibroblast- or blastema cell-derived mitogens, *in vitro* cultures have
199 shown that blastema protein extracts are able to drive blastema cell proliferation [26]. More
200 generally, a global and temporally-based view of the cellular origins of mitogens and the cell
201 types that require these mitogens will provide a better understanding of what is driving
202 proliferation during different stages of regeneration.

203 In addition to the dramatic reduction in proliferation, we observed striking end point
204 phenotypes after transient knockdown of Vwde. The loss of distal elements and spike-like
205 phenotypes observed after Vwde knockdown suggest that Vwde plays a role in proximal-distal
206 determination in the regenerating limb. These phenotypes showing similarities to *ssh* and *fgf4,8*-
207 double-knockout mice, suggest that Vwde may be working similarly to—or in concert with—
208 FGFs during regeneration. Though many FGFs are epidermal factors during limb development in
209 mice and chick, FGFs are expressed in the mesenchyme during axolotl limb development [27]
210 and regeneration [28]. Thus, it may be that during axolotl limb regeneration, blastema-derived
211 factors are primarily responsible for proximal-distal patterning and that Vwde is working to
212 promote the formation of distal elements. Intriguingly, *vwde* has remained unexplored in highly
213 studied, but less regenerative species such as mouse and human, so whether *vwde* plays a role in
214 limb development in these species is unknown.

215 It is interesting to speculate on what has been lost in amniotes that prevents appendage
216 regeneration. One possibility is genes that are lost in amniotes and present in anamniotes can
217 explain differences in regenerative capacity [29]. However, the absence of a gene in amniotes is
218 not necessarily a prerequisite when considering which candidate genes might be responsible for
219 high regenerative capacity. Alternative scenarios include, but are not limited to, genes that have
220 lost ancestral pro-regenerative function or have altered expression domains/kinetics. *Vwde* may
221 fit the paradigm of a gene that is present in both regeneration-competent and regeneration-
222 incompetent species, but may exclusively be used in the blastema, a structure that cannot be
223 produced by most regeneration-incompetent species.
224 While the blastema is required for regeneration, wound healing and activation of
225 progenitor cells required for formation of the blastema must precede blastema formation. Based
226 on the expression profile, we do not expect *vwde* to be a driver of blastema formation, but more
227 likely a downstream effector once a blastema has been established. In most cases of amputation
228 in less regenerative species, the blastema is not able to form, and thus we suspect that a more
229 upstream or systemic factor may prevent blastema formation. While there may have initially
230 been one primary cause of the loss of regenerative ability, such as the rise of adaptive immunity
231 [30] or trade-offs associated with endothermy [31], it is likely that other aspects of the
232 regenerative response have now been lost due to their lack of utility. If *vwde* played a relatively
233 specialized function in the blastema and blastemas generally do not exist in less regenerative
234 species then the use for *vwde* decreases. This could explain why 42.7% of human genomes have
235 a predicted loss-of-function copy of *VWDE*, leading to speculation that *VWDE* is potentially
236 drifting towards inactivation in the human population [32]. While the blastema remains the
237 elusive feature required for appendage regeneration, this work illustrates that taking an

evolutionarily-informed approach can lead to identification of functionally important genes. This also suggests that further work to understand the similarities between different species blastemas may help to elucidate the core molecular program of the blastema.

241 **Methods**
242
243 **Animal Experimentation**
244 All axolotl experiments were performed in accordance with Brigham and Women's Hospital
245 Institutional Animal Care and Use Committee in line with Animal Experimentation Protocol
246 #04160. All animals were bred in house, but the colony was originally derived from animals
247 obtained from Ambystoma Genetic Stock Center (Lexington, KY, NIH grant P40-OD019794).
248 For amputations, animals were narcotized in 0.1% MS-222, confirmed to be fully narcotized by
249 pinch test, amputated mid-zeugopod and the bone was trimmed. Animals were allowed to
250 recover overnight in 0.5% sulfamerazine. For all functional experiments, all four limbs were
251 amputated and injected individually. Functional experiments were performed on animals ranging
252 from 3.8-8cm.

253 *Polypterus senegalus* and *Lepidosiren paradoxa* were maintained in individual tanks in a
254 recirculating freshwater system. Animals were anesthetized before amputations: *P. senegalus* in
255 0.1% MS-222 (Sigma) and *L. paradoxa* in 0.1% clove oil diluted in the system water. Experiments
256 and animal care were performed following animal care guidelines approved by the Animal Care
257 Committee at the Universidade Federal do Para (protocol no. 037-2015). Pectoral fins in both
258 species were bilaterally amputated. For *L. paradoxa* fins were amputated at approximately 1 cm
259 distance from the body, and for *P. senegalus*, fins were amputated across the fin endoskeleton.
260 Amputated fins (regenerating and uninjured) were used for histology, *in situ* hybridization and
261 qRT-PCR analysis.

262 **Electroporation**
263 Electroporation was performed while axolotls were narcotized in 0.1% tricaine and subsequently
264 immersed in ice cold 1x PBS using a NepaGene Super Electroporator NEPA21 Type II
265 electroporator. Settings for electroporation included: 3 poring pulses at 150 Volts with a pulse
266 length of 5 milliseconds, a pulse interval of 10 milliseconds, a decay rate of 0 %, and a positive
267 (+) polarity. Transfer pulse consisted of 5 pulses at 50 Volts with a pulse length of 50 milliseconds,
268 a pulse interval of 950 milliseconds, a decay rate of 0 %, and a positive (+) polarity.

269 **qRT-PCR**.

270 Total RNA from regenerating or uninjured pectoral fins was extracted using TRIzol reagent
271 (Thermo Fisher Scientific). Residual DNA removal and RNA cleanup were performed following

272 the RNeasy Mini Kit (Qiagen) protocol. cDNA was synthesized from 0.5 µg RNA using the
273 Superscript III First-Strand Synthesis Supermix (Thermo Fisher Scientific) with oligo-dT. For
274 qPCR, amplification reactions (10 µl) prepared with the GoTaq Probe qPCR Master Mix
275 (Promega) were run in a StepOnePlus Real-Time PCR System (Applied Biosystems). Gene-
276 specific oligos (Table 3) for qRT-PCR assays were designed using Primer 3.0
277 (http://bioinfo.ut.ee/primer3/) and used in a final concentration of 200 nM to each primer. Each
278 qPCR determination was performed with three biological and three technical replicates. Relative
279 mRNA expressions were calculated with the $2^{-\Delta\Delta CT}$ method [33], using *sdha* (*P. senegalus*) or
280 *polrc1* (*L. paradoxa*) genes as endogenous control and the uninjured fin (mean ΔCT value of the
281 three biological replicates) as reference sample.

282 **In Situ Hybridization**

283 For *in situ* hybridization using axolotl samples a gene fragment from the 3' UTR was amplified
284 from blastema cDNA and cloned into the pGEM-T Easy vector and sequenced. Depending upon
285 orientation, T7 or Sp6 polymerase was used to transcribe the probe. Primers for *in situ* probes
286 against axolotl *vwde* (contig c1084387_g3_i1 from [11]) can be found in Table 3. Colorimetric
287 in situ hybridization in axolotl tissue harvested from animals with snout to tail lengths of 9.5-
288 11.5cm and was performed as previously described at protocols.io
289 (https://www.protocols.io/view/rna-in-situ-hybridization-p33dqqn).

290 For *in situ* hybridizations with fish samples, fins of *P. senegalus* (5 dpa and uninjured) and *L.*
291 *paradoxa* (21 dpa and uninjured) were amputated, embedded in TissueTek O.C.T compound
292 (Fisher Scientific), and maintained at −80°C until use. Frozen sections of 20 µm were obtained on
293 a Leica CM1850 UV cryostat, positioned on slides (Color Frost Plus/Thermo Fisher Scientific)
294 and fixed as previously described [1]. Riboprobe templates containing a gene-specific segment
295 (400-500 bp) and a T7 promoter sequence were produced by a 2-round PCR strategy (primers are
296 listed in Table 3). Riboprobes were synthesized with T7 RNA polymerase (Roche) and DIG-
297 labeling mix (Roche). Controls probes (sense riboprobes) were synthesized from a template
298 containing the T7 promoter in a reverse orientation. A total of 300 ng of DIG-labeled riboprobe
299 was used per slide during *in situ hybridization* performed as previously described [1]. Images were
300 obtained on a Nikon Eclipse 80i microscope and processed using the NIS-Element D4.10.1
301 program.

302 **Whole mount RNA-FISH**

303 *Xenopus laevis* eggs were obtained, fertilized, and cultured as embryos at 18 °C using standard
304 methods as in [34]. All experimental procedures using *Xenopus laevis* were approved by the
305 Institutional Animal Care and Use Committee (IACUC) and Tufts University Department of
306 Laboratory Animal Medicine (DLAM) under protocol number M2017-53. Once embryos reached
307 regeneration-competent (Stage 40) or regeneration-incompetent (Stage 46) stages, animals were
308 anesthetized using 0.005% MS222 in 0.1X MMR and tails were amputated at the posterior third
309 of the tail and allowed to regenerate for 24 hours. Embryos at both stages, which had not been
310 amputated, were also collected as intact controls. Regenerating and intact control embryos were
311 anesthetized in 0.005% MS222 and then fixed at 4°C, rocking overnight, in either 4%
312 paraformaldehyde in 1X DEPC PBS or MEMPA buffer (0.1 M MOPS (pH 7.4), 2 mM EGTA, 1
313 mM MgSO4, 3.7% paraformaldehyde). We used a slightly modified whole-mount mouse protocol
314 [35] using hybridization chain reaction v3.0 [36] with slight modifications. After overnight
315 incubation, embryos were washed 3 times for 5 min in PBST and then taken through a methanol
316 series on ice. This series consisted of 10 min washes on ice in ice cold 25%MeOH/75% PBST,
317 50%MeOH/50% PBST, 75%MeOH/25%PBST, 100%MeOH, and then finally stored in a fresh
318 100%MeOH solution. Dehydrated embryos were then stored at -20°C until use. For *in situ*,
319 embryos were subsequently rehydrated via a reverse methanols series, on ice, with 10 min washes
320 of 75% MeOH/25% PBST, 50% MeOH/50% PBST, 25% MeOH/75% PBST, 100% PBST, and
321 another final wash in 100% PBST. Embryos were then digested with proteinase K (10µg/mL) in
322 DEPC PBS for 5 minutes at room temperature. Post-fixation was then performed in 4% PFA in
323 1X DEPC PBS for 20 minutes at room temperature. Next, three five minutes washes with PBST
324 at room temperature was followed by 5 minutes at 37°C in hybridization solution (50% formamide,
325 5x sodium chloride sodium citrate (SSC), 9 mM citric acid (pH 6.0), 0.1% Tween-20, 50µg/mL
326 heparin, 1x Denhardt's solution, and 20% dextran sulfate). Samples were pre-hybridized by full
327 immersion in hybridization solution without probes for 30 min at 37°C. Hybridization was
328 performed overnight at 37°C with samples immersed in hybridization solution containing twenty
329 probe pairs against *vwde.L* (XM_018267342.1) diluted at 1:200 of 1 µM (hybridization chain
330 reaction v3.0 RNA fluorescent in situ probes were ordered from Molecular Instruments
331 (https://www.molecularinstruments.com/). The following day, samples were washed four times at
332 37°C in probe wash buffer (50% formamide, 5X SSC, 9 mM citric acid (pH 6.0), 0.1% Tween-20,

333 and 50µg/mL heparin). Samples were then washed two times in 5X SSC at room temperature. Pre-
334 amplification was then performed at room temperature for 30 minutes in amplification buffer (5X
335 SSC, 0.1% Tween-20, 10% dextran sulfate). During pre-amplification, hairpin probes (ordered
336 from https://www.molecularinstruments.com/) compatible with *vwde.L* probe pairs were heated
337 individually at 95°C for 30 seconds and then snap cooled for 30 min at room temperature in the
338 dark. After 30 minutes, probe pairs were added to amplification buffer at 1:50 (3 µM stock) and
339 this probe containing buffer was subsequently added to samples, ensuring that samples were fully
340 immersed. Incubation was performed overnight at room temperature. The next day, samples were
341 washed for 5 min in 5X SSCT, twice for 30 min in 5X SSCT, and a 5 min wash in 5X SSCT.
342 Samples were then stained with DAPI for 5 min in 1X PBS, washed for 5 min in 1X PBS, and then
343 stored in 1X PBS. Samples were then mounted in low melt agarose and imaged on a Zeiss LSM
344 880 Upright. A median 3x3 filter followed by maximum projection was applied to all images.

345 **Morpholino design and administration**
346 Morpholinos were designed and synthesized by GeneTools. Morpholino sequences can be found
347 in Table 3. About 1.25 µl of morpholino was injected in the blastema and electroporation was
348 performed as described in Electroporation. All morpholinos were 3' fluorescein conjugated to
349 allow for visualization. Morpholinos were reconstituted to 1 mM in 2X PBS and diluted to a
350 working concentration of 500 µM in 1X PBS prior to injection.

351
352
353 **EdU staining**
354 Stock solutions of 5-ethynyl-2'-deoxyuridine (EdU) dissolved in dimethyl sulfoxide were
355 prepared per manufacturer's instructions (Thermo Fisher). Axolotls (3-6cm tail to snout) were
356 narcotized in 0.1% tricaine at 7 days post amputation and control or Vwde-targeting morpholino
357 was injected and subsequently electroporated as described in Electroporation section of methods
358 into the blastema. At 9 dpa, intraperitoneal injections with 400 µM EdU in 0.7X PBS at a
359 volume of 20µL/g were performed. 18 hours later blastemas were harvested, fixed for 1-2h in
360 4% PFA and then taken through a sucrose gradient to 30% sucrose in 1x PBS. Tissue was then
361 embedded in OCT and frozen in a dry ice/ethanol bath. Sections were cut at 16 µm with a
362 cryostat, collected on Superfrost Plus slides (Fisher), and stored at -80°C. EdU staining was

363 performed with the Click-iT EdU Alexa Fluor 594 Imaging Kit per manufacturers instructions
364 (Thermo Fisher).
365
366 **TUNEL assay**
367 TUNEL assays were performed as previously described [11]
368
369 **Skeletal preparations and scoring**
370 Limbs were stained with Alcian blue/Alizarin red according to [37]. In brief, limbs were
371 incubated with rocking overnight in 95% ethanol and then rocking overnight an acetone. Limbs
372 were then incubated for at least 7 days in alcian blue/alizarin red at 37 °C. Limbs were then
373 cleared by incubation in 1% (wt/vol) KOH, followed by 1% (vol/vol) KOH/25% glycerol, 1%
374 KOH/50% glycerol, and 1% KOH/75% glycerol. Limbs were imaged in 1% KOH/75% glycerol.
375 Alcian blue stock was 0.3% alcian blue in 70% ethanol; alizarin red stock was 0.1% alizarin red
376 95% ethanol; the working solution was 5% alcian blue stock/5% alizarin red stock/5% glacial
377 acetic acid/volume in 70% ethanol.

378 Definitions for limbs after regeneration. Normal: All digits and carpals present, zeugopod and
379 stylopod intact. Spike: Single outgrowth from amputation plane without obvious turn at joint. Loss
380 of distal elements: Distal elements without obvious autopod. Oligodactyly: Loss or reduction in
381 size at least one digit. Syndactyly: Fusion of digits. Additional elements: Extra bones in stylopod
382 or zeugopod. For statistical analysis normal was compared to all of the above listed abnormalities.

383 **Ortholog analysis**
384 The following proteomes were downloaded from uniprot.org, human (*Homo sapiens,*
385 UP000005640, accessed 5/18/2019), zebrafish (*Danio rerio*, UP000000437, accessed
386 5/18/2019), mouse (*Mus musculus*, accessed 5/18/2019), amphioxus (*Branchiostoma floridae*,
387 accessed 8/27/2019), chick (*Gallus gallus*, accessed 8/27/2019), sea squirt (*Ciona intestinalis*,
388 accessed 8/27/2019), lamprey (*Petromyzon marinus*, accessed 8/27/2019), green anole (*Anolis*
389 *carolinensis*, 8/27/2019), frog (*Xenopus laevis*, UP000186698, accessed 7/11/2019), frog
390 (*Xenopus tropicalis*, UP000008143, accessed 7/11/2019). The South American lungfish
391 transcriptome was downloaded from https://www.ncbi.nlm.nih.gov/Traces/wgs/?val=GEHZ01
392 and converted to a putative reference protein using TransDecoder (version 5.3.0) like so:
393 `TransDecoder.LongOrfs -t`. The *Polpyterus* transcriptome can be found here:
394 https://www.ncbi.nlm.nih.gov/bioproject/480698 and converted with TransDecoder as referenced

395 above. The axolotl (*Ambystoma mexicanum*) predicted proteome was obtained from
396 https://data.broadinstitute.org/Trinity/SalamanderWeb/Axolotl.Trinity.CellReports2017.transdec
397 oder.pep.gz [11]. Cloning of axolotl *vwde* revealed a sequencing error in the axolotl
398 transcriptome which eliminated the first ~500bp of the sequence. We manually changed the
399 axolotl proteome to include this corrected version of *vwde* (Supplementary File 1).

400 To predict orthologs, we used OrthoFinder2.0 (version 2.3.3) [14]. Orthofinder was implemented
401 as follows:

402 `orthofinder -f /path/to/proteomes -M msa -A mafft  -T fasttree -t 20 -o /path/to/output/directory`

403 **Protein domain diagrams**
404 The R package, drawProteins [38] was used to draw protein domains for different species Vwde.
405 For all genes contained within Uniprot, these were downloaded directly with drawProteins. For
406 genes not available via Uniprot (https://www.uniprot.org/)[39] (e.g. *Polpyterus*, axolotl, and
407 Lungfish), the amino acid sequence of the protein was queried via Interpro with default settings
408 (https://www.ebi.ac.uk/interpro/)[40] and positions and domain annotations were extracted and
409 made into a matrix that matched the required structure for drawProteins.

410 **Vwde knockdown confirmation**
411 Two separate constructs to test the target specificity of each MO used. GFP was removed and
412 from pCAG-GFP (pCAG-GFP was a gift from Connie Cepko (Addgene plasmid # 11150 ;
413 http://n2t.net/addgene:11150 ; RRID:Addgene_11150)[41] and replaced with vectors containing
414 td-Tomato sequence and the morpholino binding site (Supplementary File 2). To confirm
415 knockdown we co-injected and electroporated into medium-bud blastemas the generated
416 constructs and the appropriate fluorescein-conjugated morpholino. Fluorescein fluorescence was
417 used to confirm injection efficiency and td-tomato expression was used to measure ability to
418 block translation.
419
420 **Statistics**
421 Nested one way ANOVA was used to determine significance between blastema lengths. Each
422 limb was considered a technical replicate within one biological (i.e. animal) replicate. Nested t
423 tests were used to determine significance in EdU and TUNEL experiments, again treating each
424 limb as a technical replicate and placing limbs from the same animal within one biological

425 replicate. Fisher's exact tests (control vs. treated) were used to determine significance of
426 outgrowth phenotypes. Significant results were considered as $P < 0.05$.

427 **Contributions**

	NDL	SS	ACD	DPD	JFS	ANA	KJ	GSD	BJH	ML	IS	JLW
Wrote the paper	■											■
Initiation/conception	■								■			■
Corresponding author												■
Animal experiments/in situ	■	■	■	■	■	■	■	■		■		■
Orthology analysis	■											
Experimental design	■	■	■	■	■			■			■	■
Manuscript editing	■	■	■	■	■	■	■	■	■	■	■	■
Contributed resources											■	■

428

Acknowledgements

This work was supported by the Eunice Kennedy Shriver National Institute of Child and Human Development of the National Institutes of Health (5R03HD083434-02 to J.L.W.). N.D.L. was supported by Award Number F32HD092120 from the Eunice Kennedy Shriver National Institute of Child and Human Development of the National Institutes of Health. Portions of this research were conducted on the O2 High Performance Compute Cluster, supported by the Research Computing Group, at Harvard Medical School. See http://rc.hms.harvard.edu for more information. Support for work on lungfish and *Polypterus* was provided by CNPq Universal Program Grant 403248/2016-7 and CAPES/DAAD PROBRAL Grant 88881.198758/2018-01 to I.S, and a postdoctoral fellowship from CNPq to A.C.D. We thank William Ye, Adam Gramy, Sarah Lemire, and Bonney Couper-Kiablick for expert animal care and other members of the Whited lab for feedback and discussions. We also thank Dr. Mansi Srivastava and Dr. Ryan Walker for their insights on orthology and protein structure and Dr. James Monaghan and Timothy Duerr for sharing information on whole mount in situ protocols.

443 **References**

444 1. Nogueira, A.F., Costa, C.M., Lorena, J., Moreira, R.N., Frota-Lima, G.N., Furtado, C.,
445 Robinson, M., Amemiya, C.T., Darnet, S., and Schneider, I. (2016). Tetrapod limb and
446 sarcopterygian fin regeneration share a core genetic programme. Nat. Commun. *7*, 13364.

447 2. Darnet, S., Dragalzew, A.C., Amaral, D.B., Sousa, J.F., Thompson, A.W., Cass, A.N.,
448 Lorena, J., Pires, E.S., Costa, C.M., Sousa, M.P., *et al.* (2019). Deep evolutionary origin of
449 limb and fin regeneration. Proc. Natl. Acad. Sci. U. S. A. *116*, 15106–15115.

450 3. Fröbisch Nadia B., Bickelmann Constanze, and Witzmann Florian (2014). Early evolution
451 of limb regeneration in tetrapods: evidence from a 300-million-year-old amphibian.
452 Proceedings of the Royal Society B: Biological Sciences *281*, 20141550.

453 4. Fröbisch, N.B., Bickelmann, C., Olori, J.C., and Witzmann, F. (2015). Deep-time evolution
454 of regeneration and preaxial polarity in tetrapod limb development. Nature *527*, 231–234.

455 5. Voss, S.R., Palumbo, A., Nagarajan, R., Gardiner, D.M., Muneoka, K., Stromberg, A.J., and
456 Athippozhy, A.T. (2015). Gene expression during the first 28 days of axolotl limb
457 regeneration I: Experimental design and global analysis of gene expression. Regeneration
458 (Oxf) *2*, 120–136.

459 6. Knapp, D., Schulz, H., Rascon, C.A., Volkmer, M., Scholz, J., Nacu, E., Le, M.,
460 Novozhilov, S., Tazaki, A., Protze, S., *et al.* (2013). Comparative transcriptional profiling
461 of the axolotl limb identifies a tripartite regeneration-specific gene program. PLoS One *8*,
462 e61352.

463 7. Stewart, R., Rascon, C.A., Tian, S., Nie, J., Barry, C., Chu, L.F., Ardalani, H., Wagner, R.J.,
464 Probasco, M.D., Bolin, J.M., *et al.* (2013). Comparative RNA-seq analysis in the
465 unsequenced axolotl: the oncogene burst highlights early gene expression in the blastema.
466 PLoS Comput. Biol. *9*, e1002936.

467 8. Monaghan, J.R., Athippozhy, A., Seifert, A.W., Putta, S., Stromberg, A.J., Maden, M.,
468 Gardiner, D.M., and Voss, S.R. (2012). Gene expression patterns specific to the
469 regenerating limb of the Mexican axolotl. Biol. Open *1*, 937–948.

470 9. Monaghan, J.R., Epp, L.G., Putta, S., Page, R.B., Walker, J.A., Beachy, C.K., Zhu, W., Pao,
471 G.M., Verma, I.M., Hunter, T., *et al.* (2009). Microarray and cDNA sequence analysis of
472 transcription during nerve-dependent limb regeneration. BMC Biol. *7*, 1.

473 10. Wu, C.H., Tsai, M.H., Ho, C.C., Chen, C.Y., and Lee, H.S. (2013). De novo transcriptome
474 sequencing of axolotl blastema for identification of differentially expressed genes during
475 limb regeneration. BMC Genomics *14*, 434.

476 11. Bryant, D.M., Johnson, K., DiTommaso, T., Tickle, T., Couger, M.B., Payzin-Dogru, D.,
477 Lee, T.J., Leigh, N.D., Kuo, T.-H., Davis, F.G., *et al.* (2017). A Tissue-Mapped Axolotl De
478 Novo Transcriptome Enables Identification of Limb Regeneration Factors. Cell Rep. *18*,
479 762–776.

480 12. Leigh, N.D., Dunlap, G.S., Johnson, K., Mariano, R., Oshiro, R., Wong, A.Y., Bryant,
481 D.M., Miller, B.M., Ratner, A., Chen, A., *et al.* (2018). Transcriptomic landscape of the
482 blastema niche in regenerating adult axolotl limbs at single-cell resolution. Nat. Commun.
483 *9*, 5153.

484 13. Gerber, T., Murawala, P., Knapp, D., Masselink, W., Schuez, M., Hermann, S., Gac-Santel,
485 M., Nowoshilow, S., Kageyama, J., Khattak, S., *et al.* (2018). Single-cell analysis uncovers
486 convergence of cell identities during axolotl limb regeneration. Science *362*. Available at:
487 http://dx.doi.org/10.1126/science.aaq0681.

488 14. Emms, D.M., and Kelly, S. (2018). OrthoFinder2: fast and accurate phylogenomic
489 orthology analysis from gene sequences. biorxiv. Available at:
490 https://www.biorxiv.org/content/biorxiv/early/2018/11/08/466201.full.pdf.

491 15. Shubin, N., Tabin, C., and Carroll, S. (1997). Fossils, genes and the evolution of animal
492 limbs. Nature *388*, 639–648.

493 16. Beck, C.W., Christen, B., and Slack, J.M.W. (2003). Molecular pathways needed for
494 regeneration of spinal cord and muscle in a vertebrate. Dev. Cell *5*, 429–439.

495 17. Mariani, F.V., Ahn, C.P., and Martin, G.R. (2008). Genetic evidence that FGFs have an
496 instructive role in limb proximal-distal patterning. Nature *453*, 401–405.

497 18. Chiang, C., Litingtung, Y., Lee, E., Youngt, K.E., Cordent, J.L., Westphal, H., and Beachyt,
498 P.A. Cyclopia and defective axial patterning in mice lacking Sonic hedgehog gene function.
499 Available at: https://www-nature-com.ezp-prod1.hul.harvard.edu/articles/383407a0.pdf.

500 19. Dent, J.N. (1962). Limb Regeneration in Larvae and Metamorphosing Individuals of the
501 South African Clawed Toad. Journal of Morphology *110*, 61–77.

502 20. Mescher, A.L., and Tassava, R.A. (1975). Denervation effects on DNA replication and
503 mitosis during the initiation of limb regeneration in adult newts. Dev. Biol. *44*, 187–197.

504 21. Johnson, K., Bateman, J., DiTommaso, T., Wong, A.Y., and Whited, J.L. (2017). Systemic
505 cell cycle activation is induced following complex tissue injury in axolotl. Dev. Biol.
506 Available at: https://www.ncbi.nlm.nih.gov/pubmed/29111100.

507 22. Farkas, J.E., Freitas, P.D., Bryant, D.M., Whited, J.L., and Monaghan, J.R. (2016).
508 Neuregulin-1 signaling is essential for nerve-dependent axolotl limb regeneration.
509 Development *143*, 2724–2731.

510 23. Brockes, J.P., and Kintner, C.R. (1986). Glial growth factor and nerve-dependent
511 proliferation in the regeneration blastema of Urodele amphibians. Cell *45*, 301–306.

512 24. Sugiura, T., Wang, H., Barsacchi, R., Simon, A., and Tanaka, E.M. (2016). MARCKS-like
513 protein is an initiating molecule in axolotl appendage regeneration. Nature *531*, 237–240.

514 25. Endo, T., Bryant, S.V., and Gardiner, D.M. (2004). A stepwise model system for limb

515 regeneration. Dev. Biol. *270*, 135–145.

516 26. Boilly, B., and Albert, P. (1990). In vitro control of blastema cell proliferation by extracts
517 from epidermal cap and mesenchyme of regenerating limbs of axolotls. Rouxs. Arch. Dev.
518 Biol. *198*, 443–447.

519 27. Purushothaman, S., Elewa, A., and Seifert, A.W. (2019). Fgf-signaling is
520 compartmentalized within the mesenchyme and controls proliferation during salamander
521 limb development. Elife *8*. Available at: http://dx.doi.org/10.7554/eLife.48507.

522 28. Nacu, E., Gromberg, E., Oliveira, C.R., Drechsel, D., and Tanaka, E.M. (2016). FGF8 and
523 SHH substitute for anterior-posterior tissue interactions to induce limb regeneration. Nature
524 *533*, 407–410.

525 29. Korotkova, D.D., Lyubetsky, V.A., Ivanova, A.S., Rubanov, L.I., Seliverstov, A.V.,
526 Zverkov, O.A., Martynova, N.Y., Nesterenko, A.M., Tereshina, M.B., Peshkin, L., *et al.*
527 (2019). Bioinformatics Screening of Genes Specific for Well-Regenerating Vertebrates
528 Reveals c-answer, a Regulator of Brain Development and Regeneration. Cell Rep. *29*,
529 1027–1040.e6.

530 30. Godwin, J.W., Pinto, A.R., and Rosenthal, N.A. (2017). Chasing the recipe for a pro-
531 regenerative immune system. Semin. Cell Dev. Biol. *61*, 71–79.

532 31. Hirose, K., Payumo, A.Y., Cutie, S., Hoang, A., Zhang, H., Guyot, R., Lunn, D., Bigley,
533 R.B., Yu, H., Wang, J., *et al.* (2019). Evidence for hormonal control of heart regenerative
534 capacity during endothermy acquisition. Science *364*, 184–188.

535 32. MacArthur, D.G., Balasubramanian, S., Frankish, A., Huang, N., Morris, J., Walter, K.,
536 Jostins, L., Habegger, L., Pickrell, J.K., Montgomery, S.B., *et al.* (2012). A systematic
537 survey of loss-of-function variants in human protein-coding genes. Science *335*, 823–828.

538 33. Livak, K.J., and Schmittgen, T.D. (2001). Analysis of relative gene expression data using
539 real-time quantitative PCR and the 2(-Delta Delta C(T)) Method. Methods *25*, 402–408.

540 34. Sive, H.L., Grainger, R.M., and Harland, R.M. (2010). Early Development of Xenopus
541 Laevis by Hazel L Sive, Robert M Grainger | Waterstones. Available at:
542 https://www.waterstones.com/book/early-development-of-xenopus-laevis/hazel-l-
543 sive//9780879699420 [Accessed November 12, 2019].

544 35. Choi, H.M.T., Calvert, C.R., Husain, N., Huss, D., Barsi, J.C., Deverman, B.E., Hunter,
545 R.C., Kato, M., Lee, S.M., Abelin, A.C.T., *et al.* (2016). Mapping a multiplexed zoo of
546 mRNA expression. Development *143*, 3632–3637.

547 36. Choi, H.M.T., Schwarzkopf, M., Fornace, M.E., Acharya, A., Artavanis, G., Stegmaier, J.,
548 Cunha, A., and Pierce, N.A. (2018). Third-generation in situ hybridization chain reaction:
549 multiplexed, quantitative, sensitive, versatile, robust. Development *145*. Available at:
550 http://dx.doi.org/10.1242/dev.165753.

551 37. Whited, J.L., Lehoczky, J.A., and Tabin, C.J. (2012). Inducible genetic system for the
552 axolotl. Proc. Natl. Acad. Sci. U. S. A. *109*, 13662–13667.

553 38. Brennan, P. (2018). drawProteins: a Bioconductor/R package for reproducible and
554 programmatic generation of protein schematics. F1000Res. *7*, 1105.

555 39. UniProt Consortium (2019). UniProt: a worldwide hub of protein knowledge. Nucleic Acids
556 Res. *47*, D506–D515.

557 40. Hunter, S., Apweiler, R., Attwood, T.K., Bairoch, A., Bateman, A., Binns, D., Bork, P.,
558 Das, U., Daugherty, L., Duquenne, L., *et al.* (2009). InterPro: the integrative protein
559 signature database. Nucleic Acids Res. *37*, D211–5.

560 41. Matsuda, T., and Cepko, C.L. (2004). Electroporation and RNA interference in the rodent
561 retina in vivo and in vitro. Proc. Natl. Acad. Sci. U. S. A. *101*, 16–22.

562 **Figure Legends**

563

564

565 **Figure 1: *von Willebrand Factor D and EGF-like Domains* (*vwde*) is a blastema-enriched**
566 **gene that is found across deuterostomes.** (A) *vwde* (contig c1084387_g3_i1) expression in
567 FPKM across tissues sampled from Bryant et al. Cell Reports 2017. Proximal and distal blastema
568 samples are combined. (B-E) RNA *in situ* hybridization for *vwde* at (B) wound healing, (C)
569 early-bud blastema, (D) medium-bud blastema, and (E) palette stage regenerating limbs. Black
570 arrows indicate *vwde* expression, scale bar is 100 µm. (F) OrthoFinder 2.0 phylogeny with
571 corresponding protein domain structure for putative Vwde orthologs. Protein domain pictures
572 were generated with drawProteins [38]. Species and Uniprot ID or transcriptome contig number
573 are included. *Polypterus vwde* contained multiple splice isoforms and the closest match to axolotl
574 Vwde is shown here. Axolotl Vwde is denoted with (*) and other species Vwde that are
575 described in this manuscript are marked with (#). Orthologs to the Vwde studied in this work are
576 indicated with brackets, paralog is also denoted with brackets.
577

578 **Figure 2: *vwde* is enriched in the regenerating fin of Lungfish (*L. paradoxa*) and *Polypterus***
579 **(*P. senegalus*).** Expression pattern of *vwde* in the fin blastema tissues *of L. paradoxa* and *P.*
580 *senegalus*. Longitudinal histological sections of fins from *L. paradoxa* at 21 dpa (A-B), and from
581 *P. senegalus* at 5 dpa (C-D). (A and C) *In situ* hybridization using an anti-sense riboprobe to
582 *vwde*. (B and D) H&E staining on sequential sections. All panels show posterior view, dorsal to
583 the top. Dotted lines indicate amputation site (Scale bars, 1 mm in all panels).
584

585 **Figure 3: *vwde* expression is tightly linked with the regeneration-component environment.**
586 *In situ* hybridization chain reaction probing for *vwde* in (A-F) regeneration-competent *Xenopus*
587 *laevis* tails (A-B) prior to amputation, (C-D) blastema 24 hours post-amputation, and (E-F) the
588 peripheral edge of the amputation plane 24 hours post-amputation. (G-L) Regeneration-
589 refractory tails (G-H) prior to amputation, (I-J) blastema 24 hours post-amputation, and (K-L)
590 the peripheral edge of the amputation plane 24 hours post-amputation. White arrows indicate the
591 location of *vwde* expression. Scale bars are 100 µm.

592
593 **Figure 4: Vwde is essential for limb regeneration.** (A) Representative images of blastemas 16
594 days post-amputation (9 days post-morpholino administration) from control morpholino
595 (Standard control MO), *vwde*-targeting morpholino 1 (*vwde* MO1), and *vwde*-targeting
596 morpholino 2 (*vwde* MO2). Dotted line indicates amputation plane, blastemas are all tissue distal
597 to amputation plane. Scale bars at 1mm. (B) Quantification of blastema length 16 days-post
598 amputation. Median and quartiles noted with dotted lines, ** indicates P< 0.01, * is P< 0.05 by
599 nested T test. (C) Representative EdU stained sections of blastemas 10 dpa (3 days post-
600 electroporation) of control morpholino (*vwde* morpholino 1 inverted, *vwde* MO1 INV) and *vwde*-
601 targeting morpholino 1. Scale bars are 100µm (D) Quantification of percent of blastema cells
602 positive for EdU in control (*vwde* MO1 INV) and knockdown (*vwde* MO1). Each dot represents
603 a limb, 4-5 animals per group. Median and quartiles noted with dotted lines,** indicates P< 0.01
604 by nested T test. (E) Representative skeletal preparations of limbs after full regeneration after
605 knockdown of Vwde at 7 dpa. From left to right, normal forelimb, normal hindlimb, spike, and
606 loss of distal elements. Scale bars are 5 mm. (F) Donut plots of regenerative outcomes, pooled as
607 abnormal versus normal from experiment with standard control morpholino, *vwde* MO1 and
608 *vwde* MO2. Asterisk (*) indicates P< 0.05 by Fisher's exact test comparing control versus *vwde*
609 MO1 and control versus *vwde* MO2. (G) Donut plots of regenerative outcomes, pooled as
610 abnormal versus normal from experiment with *vwde* MO1 INV and *vwde* MO1. Asterisk (*)
611 indicates P< 0.05 by Fisher's exact test comparing outcomes from *vwde* MO1 INV compared to
612 *vwde* MO1.

613 Table 1. Phenotypic outcomes of morpholino-mediated knockdown in axolotl (Standard control
614 vs. *vwde* MO1, *vwde* MO2)

	Normal	Spike	Loss of distal elements	Oligodactyly	Polydactyly	Syndactyly	Additional elements
Control	23	0	0	0	0	1	0
vwde MO1	15	4	5	4	0	0	0
vwde MO2	11	0	0	3	1	1	0

615

616

617 Table 2. Phenotypic outcomes of morpholino-mediated knockdown in axolotl (Inverted control vs.
618 *vwde* MO1)

	Normal	Spike	Loss of distal elements	Oligodactyly	Polydactyly	Syndactyly	Additional elements
Vwde MO1 INV	30	0	4	4	0	0	0
Vwde MO1	20	6	9	1	0	1	1

619

620

621

622

623

624

625

626

627

628

629 Table 3. Oligos used for qPCR, morpholinos, and ISH probe templates.

Primer	Application	Sequence (5'- 3')
Ax_vwde_ISH_F	Riboprobe template	TGTGGAAAGAAACTTGTGCATCA
Ax_vwde_ISH_R	Riboprobe template	TTTAATCTGAAAATGGACCAGTAGATT
vwde MO1	Anti-sense morpholino	ATATCCCATACATCCTTGCGTTGGC
vwde MO2	Anti-sense morpholino	AGAAACCATCACAGTTCCTCACAGT
vwde MO1 INV	Sense (control) morpholino	CGGTTGCGTTCCTACATACCCTATA
Standard control MO	Control morpholino	CCTCTTACCTCAGTTACAATTTATA
Ps_Vwde-qPCR_F	qPCR	AGAATTCCTGTGACTGTGCGA
Ps_Vwde-qPCR_R	qPCR	TTCTGGTGTTGTTGGTGAGGG
Ps_Vwde-ISH_F	Riboprobe template	GGCCGCGGGCATGCGGAATAATGTGTGCT
Ps_Vwde-ISH_R	Riboprobe template	CCCGGGGCAGTCCAGTCTTCAGCAGTGTG
Lp_Vwde-qPCR_F	qPCR	TTCTTCTTGGAGACCCCTGAT
Lp_Vwde-qPCR_R	qPCR	GGTCTTGCTGGCTAGTGTCAG
Lp_Vwde-ISH_F	Riboprobe template	GGCCGCGGAGCTAACAGCCTGTGCAACAT
Lp_Vwde-ISH_R	Riboprobe template	CCCGGGGCATCAGGGGTCTCCAAGAAGAA
3'_T7 universal	Riboprobe template, 2nd-round PCR	AGGGATCCTAATACGACTCACTATAGGGCC CGGGGC
5'_T7 universal	Riboprobe template, 2nd-round PCR	GAGAATTCTAATACGACTCACTATAGGGCC GCGG

630

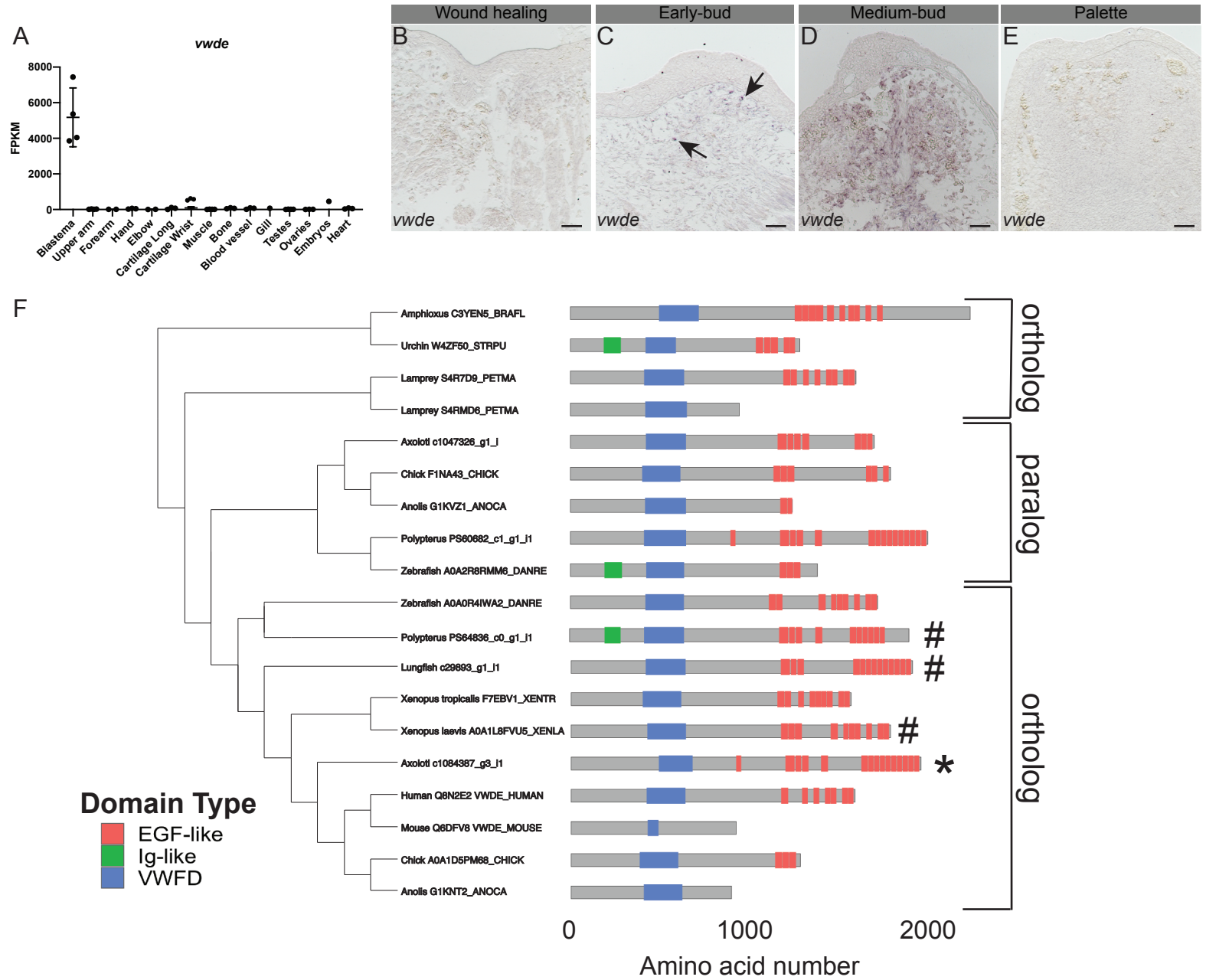
A
vwde
FPKM
8000
6000
4000
2000
0
Blastema
Upper arm
Forearm
Hand
Elbow
Cartilage Long
Cartilage Wrist
Muscle
Bone
Blood vessel
Gill
Testes
Ovaries
Embryos
Heart
Wound healing
Early-bud
Medium-bud
Palette
B
C
D
E
vwde
F
Amphioxus C3YEN5_BRAFL
Urchin W4ZF50_STRPU
Lamprey S4R7D9_PETMA
Lamprey S4RMD6_PETMA
Axoloti c1047326_g1_i
Chick F1NA43_CHICK
Anolis G1KVZ1_ANOCA
Polypterus PS60682_c1_g1_i1
Zebrafish A0A2R8RMM6_DANRE
Zebrafish A0A0R4IWA2_DANRE
Polypterus PS64836_c0_g1_i1
Lungfish c29893_g1_i1
Xenopus tropicalis F7EBV1_XENTR
Xenopus laevis A0A1L8FVU5_XENLA
Axoloti c1084387_g3_i1
Human Q8N2E2 VWDE_HUMAN
Mouse Q6DFV8 VWDE_MOUSE
Chick A0A1D5PM68_CHICK
Anolis G1KNT2_ANOCA
ortholog
paralog
ortholog
#
#
#
*
Domain Type
EGF-like
Ig-like
VWFD
0
1000
2000
Amino acid number

Figure 2

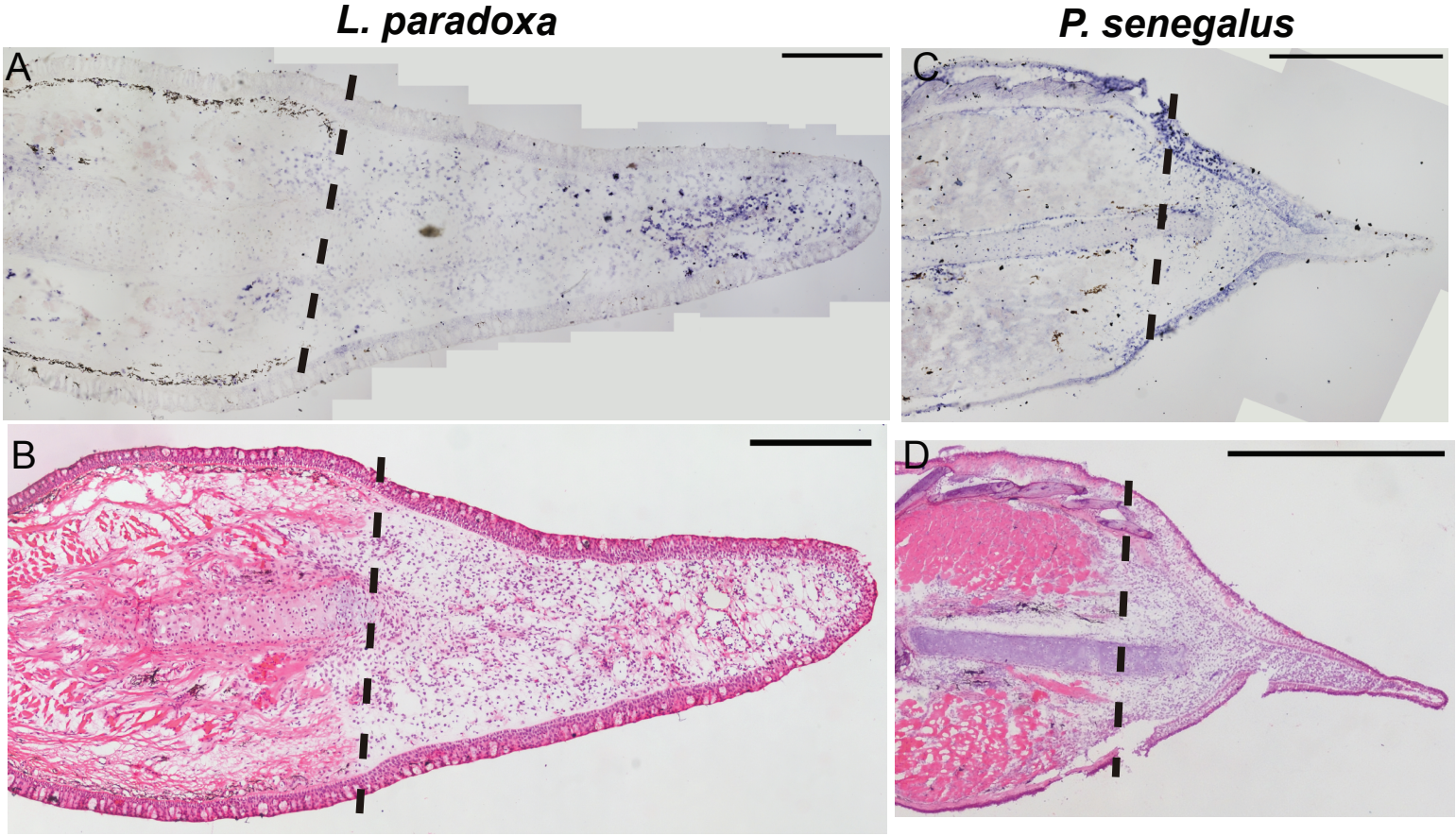

Figure 3

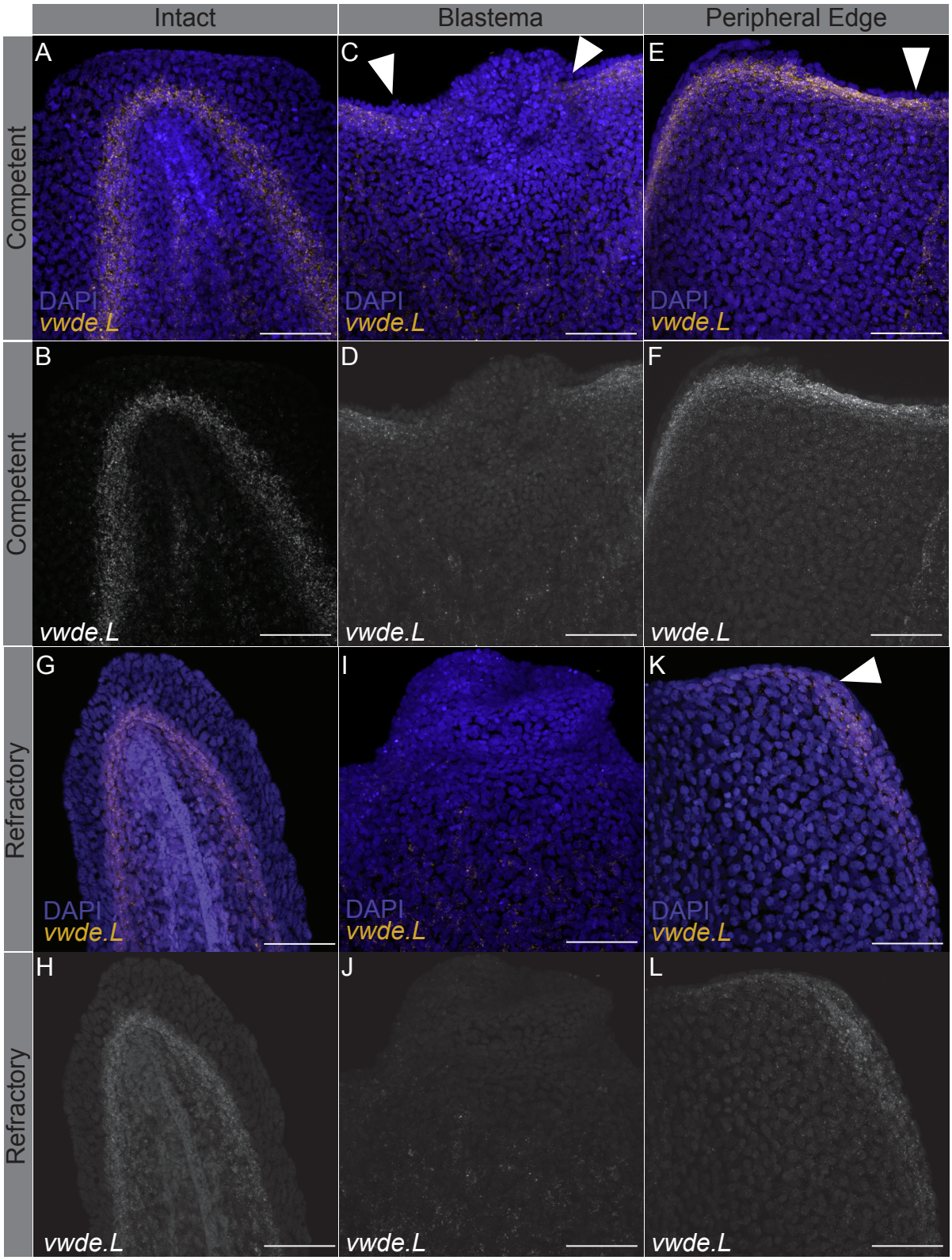
Intact
Blastema
Peripheral Edge
Competent
Competent
Refractory
Refractory
A
B
C
D
E
F
G
H
I
J
K
L
DAPI
vwde.L

Figure 4

A

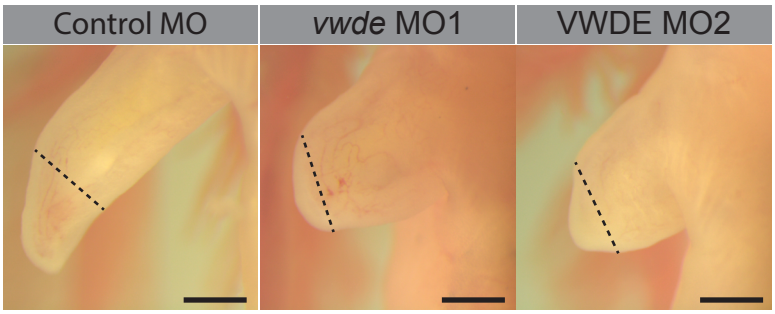

B

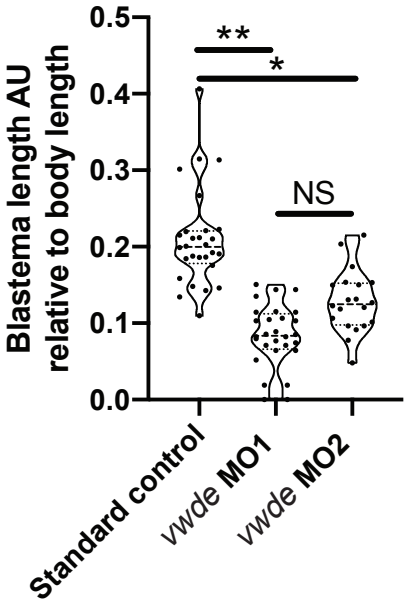

C

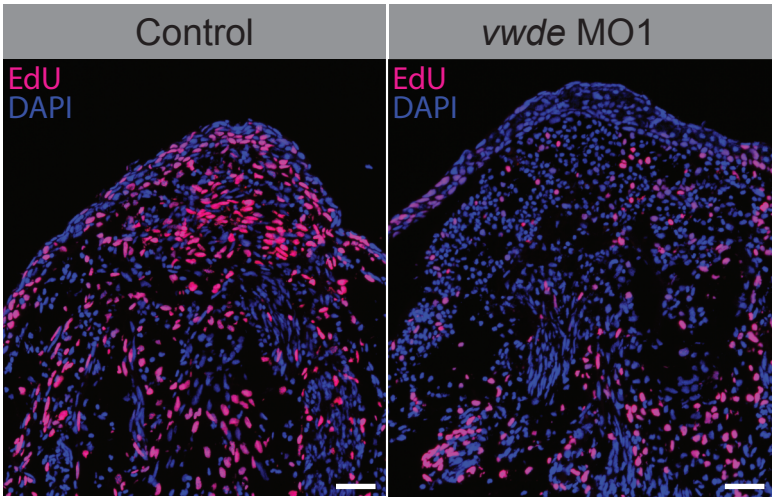

D

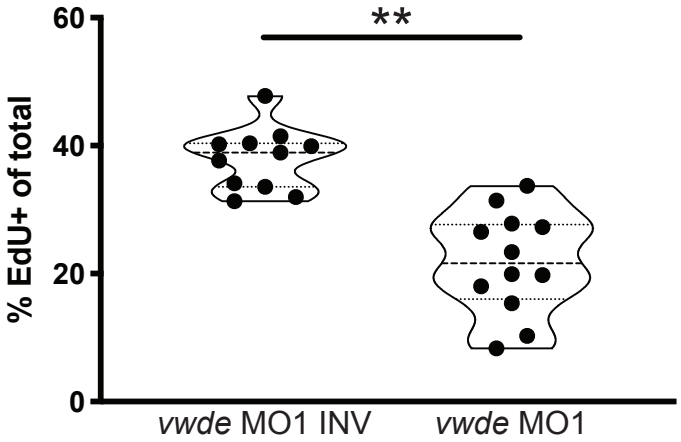

E

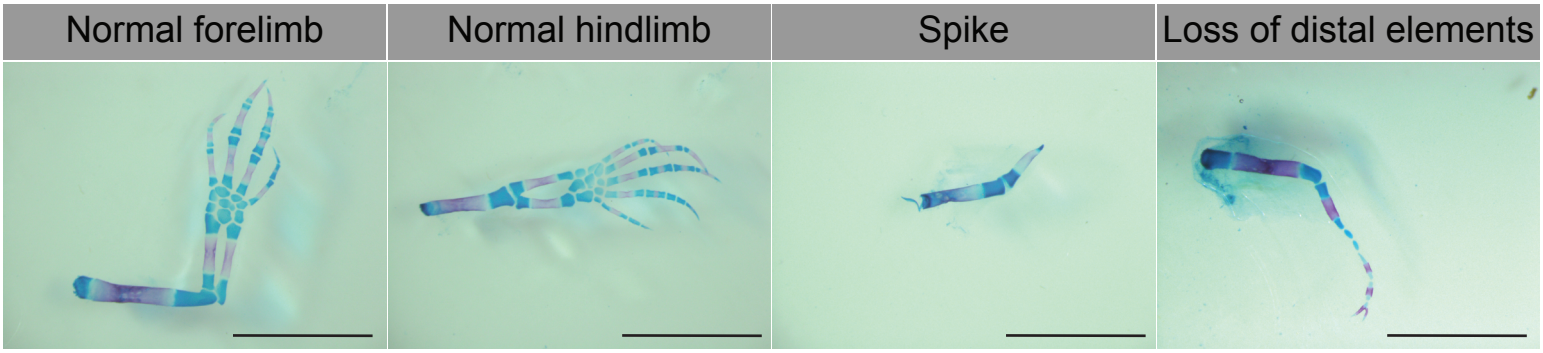

F

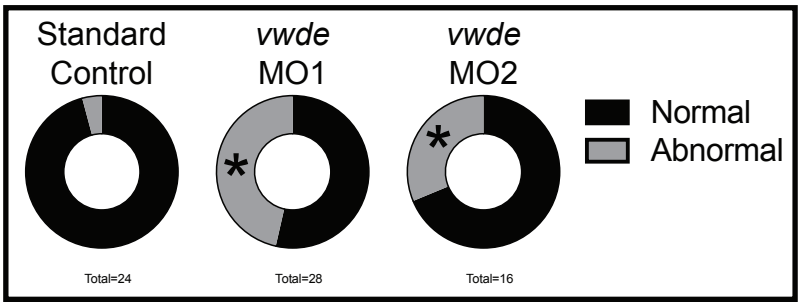
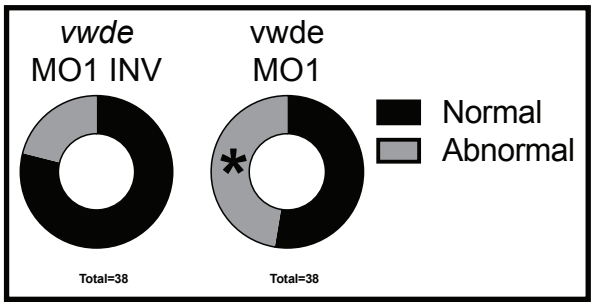
G